Canadian Science Publishing | Canadian Journal of Chemistry

Thermal kinetics, thermodynamics, decomposition mechanism, and thermal safety performance of typical ammonium perchlorate-based molecular perovskite energetic materials

Journal:	*Canadian Journal of Chemistry*
Manuscript ID	cjc-2021-0223.R1
Manuscript Type:	Article
Date Submitted by the Author:	26-Oct-2021
Complete List of Authors:	An, Erhai; North University of China, School of environmental and safety engineering Chen, Shaoli; Xi'an Modern Chemistry Research Institute Li, Xiaoxia; North University of China Hu, Lishuang; North University of China Tan, Yingxin; North University of China Cao, Xiong; North University of China Deng, Peng; North University of China; Beijing Institute of Technology
Is the invited manuscript for consideration in a Special Issue? :	Not applicable (regular submission)
Keyword:	

SCHOLARONE™
Manuscripts

© The Author(s) or their Institution(s)

Thermal kinetics, thermodynamics, decomposition mechanism, and thermal safety performance of typical ammonium perchlorate-based molecular perovskite energetic materials

Erhai An[†], Shaoli Chen[‡], Xiaoxia Li[†], Yingxin Tan*[,†], Xiong Cao[†], and Peng Deng*[,†,§]

[†] School of Environment and Safety Engineering, North University of China, Taiyuan 030051, Shanxi, People's Republic of China

[‡] Xi'an Modern Chemistry Research Institute, Xi'an 710065, Shaanxi, People's Republic of China

[§] State Key Laboratory of Explosion Science and Technology, Beijing Institute of Technology, Beijing 100081, People's Republic of China

Corresponding Author

* Tel: +86 0351 3920630. Fax: +86 0351 3920630. E-mail: TanYXnuc@163.com (Y. T).

*Tel: +86 0351 3920630. Fax: +86 0351 3920630. E-mail: nash_deng@163.com (P. D).

Draft

© The Author(s) or their Institution(s)

Abstract: In this work, we reported that the thermal kinetics, thermodynamics, and decomposition mechanism of AP-based molecular perovskite energetic materials were studied, and their thermal safety performance was estimated. Typical AP-based molecular perovskite energetic materials $(H_2dabco)[NH_4(ClO_4)_3]$ (DAP-4), $(H_2pz)[NH_4(ClO_4)_3]$(PAP-4), $(H_2mpz)[NH_4(ClO_4)_3]$(PAP-M4), and $(H_2hpz)[NH_4(ClO_4)_3]$ (PAP-H4) were synthesized and characterized. These were studied by differential scanning calorimetry (DSC). The results show all of the obtained AP-based molecular perovskite energetic materials have higher thermal decomposition temperatures, and the peak temperatures are more than 360 °C. And all follow the random nucleation and growth model. Other thermodynamic parameters, such as reaction enthalpy (ΔH), entropy change (ΔS), and Gibbs free energy (ΔG) show that they are generally thermodynamically stable. Moreover, their adiabatic induced temperatures were obtained, T_{D24} of DAP-4, PAP-4, PAP-M4, and PAP-H4 are 246.6, 201.2, 194.5, and 217.5°C, respectively. The work offered an important and in-depth understanding for the thermal decomposition characteristics of AP-based molecular perovskite energetic materials and their potential applications.

Draft

Keywords：AP-based molecular perovskite energetic materials, DAP-4, Thermal kinetics, thermal safety performance

© The Author(s) or their Institution(s)

1. Introduction

In recent years, with the increase of the functional requirements of energetic materials in the fields of civilian and military applications, energetic materials with unique and excellent characteristics have attracted widespread attention all over the world[1-2]. At present, the mainstream energetic materials are cyclotetramethylenetetranitramine (HMX), hexanitrohexaazaisowurtzitane (CL-20), and so on. But balancing contradictions between their safety and detonation performance still existed. Due to poor thermal stability of ammonium nitrate explosives, it is difficult to realize their multifunctional applications, although the energy level of all is high. For example, the density of ε-CL-20 is 2.04 $g \cdot cm^{-3}$, which has high explosion velocity of 9.66 $km \cdot s^{-1}$. It is considered as a promising energetic material with the highest density and energy[3]. However, its impact sensitivity is 26.8 cm and even initial decomposition temperature is below 210 °C[4-5]. And 1,3,5-triamino-2,4,6-trinitrobenzene (TATB) is one of the most insensitive explosives, its shock wave sensitivity is 124 cm and impact sensitivity is more than 320 cm, and thermal decomposition temperature is above 360 °C, which can be seen that it has excellent thermal stability and safety[6]. However, it's density is as low as 1.93 $g \cdot cm^{-3}$ and the detonation velocity is only 7.60 $km \cdot s^{-1}$ [7]. To the best of our knowledge, for most traditional high-energy compounds, the coexistence of good explosive performance and thermal stability seem to be difficult. Therefore, it is very urgent and meaningful to find a new structural energetic compound with outstanding advantages, and to explore its application possibilities to meet the needs of practical application at the extreme and complicated environment.

Chen's group firstly reported that a class of novel high-energy-density materials with molecular perovskite structure[8], which showed excellent thermal stability and detonation performance, as well as good cost advantage and production process[9-12]. Among them, the most representative one is $(H_2dabco)[NH_4(ClO_4)_3]$ (DAP-4) among AP-based molecular perovskite energy materials[13-15]. DAP-4 has a crystal density of 1.87 $g \cdot cm^{-3}$. The measured explosion heat value is 5.69 $kJ \cdot g^{-1}$ and the measured explosion velocity is higher than 8.5 $km \cdot s^{-1}$. The initial thermal decomposition

© The Author(s) or their Institution(s)

temperature is 360 °C, and the thermal decomposition peak temperature is higher than 400 °C. Compared from the existing high heat resistant explosive hexanitrostilbene (HNS), DAP-4 showed good stability and compatibility[16-26].

However, due to the short time of appearance, there is not enough understanding of the properties of the substance and the nature of the substance itself, especially in terms of thermal decomposition and thermal safety of energetic materials[27]. As we all know, the thermal behavior of energetic materials will directly affect its safe production, storage and use. It is one of the most important properties of energetic materials, and thermal analysis kinetics can quickly and easily evaluate the thermal behavior of energetic materials[28-36]. In the past few decades, CL-20[37-39], HMX[40-43], 1,1-diamino-2,2-dinitroethene (FOX-7)[44-45], Dihydroxylammonium 5,5′-bistetrazole-1,1′-diolate (TKX-50)[46-49], and 2,6-Diamino-3,5-dinitropyrazine-1-oxide (LLM-105)[50-51] are mainly studied to understand the intrinsic properties of their thermal decomposition progresses of explosives. For example, Djalal Trache et.al investigated the effect of porosity of ammonium perchlorate (AP) on thermodynamic and thermal properties of ammonium perchlorate/polyvinyl chloride (PVC) composite propellant by using the isoconversional methods[52]. Our group reported previously that a decoupling analysis of the exothermic peak of TKX-50 was conducted and found that the decomposition reaction in the first stage has autocatalytic performance[47], and suggested that it should be avoided in an adiabatic environment and used in industrial production and storage processes. It is necessary to avoid the storage of large amounts of TKX-50 and keep the heat source away from the storage location. Therefore, it is very urgent to systematically evaluate the thermal kinetics, thermodynamics, and decomposition mechanism of AP-based molecular perovskite energetic materials.

In this work, four typical AP-based molecular perovskite energetic materials $(H_2dabco)[NH_4(ClO_4)_3]$ (DAP-4), $(H_2pz)[NH_4(ClO_4)_3]$ (PAP-4), $(H_2mpz)[NH_4(ClO_4)_3]$ (PAP-M4), and $(H_2hpz)[NH_4(ClO_4)_3]$ (PAP-H4) were selected to conduct a comprehensive study of these kinds of compounds. Firstly, DSC data was collected to study the kinetics, thermodynamics, and decomposition mechanism of four AP-based molecular perovskite energetic materials. And, coupling QMS technique was used to

Draft

© The Author(s) or their Institution(s)

verify their thermal decomposition mechanism. Finally, based on the thermal analysis software AKTS, the specific heat capacity parameters and simulated their adiabatic induction temperature (TMR_{ad}) were assessed. This work offered a new understanding of thermal decomposition characteristics of AP-based molecular perovskite energetic materials.

Draft

© The Author(s) or their Institution(s)

2. EXPERIMENTAL SECTION

2.1 Materials

Perchloric acid (70%) and raw powder ammonium perchlorate (AP) were provided by Shanxi Jiangyang Chemical Technology Co., Ltd. Triethylenediamine(dacbo), piperazine, homo-piperazine, 1-methylpiperazine, and ethanol are provided by Shanghai Aladdin Biochemical Technology Co., Ltd. Deionized water is made in our laboratory.

2.2 Preparation of DAP-4, PAP-4, PAP-M4, and PAP-H4

DAP-4, PAP-4, PAP-M4, and PAP-H4 were synthesized according to literature methods[13]. 2 ml $HClO_4$, 1 mmol dabco, and 1 mmol AP were added into 40 mL deionized water, heating to 50℃ and stirring for 30 mins, and then cool naturally. And the solution was filtered. The filtered sample was dried in an oven to obtain the dried DAP-4 samples.

3 ml $HClO_4$, 2 mmol AP, and 2 mmol piperazine were added into 5 mL deionized water, heating to 80℃ and stirring for 30 mins, and then cool naturally. The filtered sample was dried to obtain dried PAP-4 samples.

1.4 ml $HClO_4$, 2 mmol AP, and 2 mmol 1-methylpiperazine (homopiperazine) was add into 5 mL distilled water, heating and stirring for 30 mins, and then cool naturally. After filtering and drying, PAP-M4 (PAP-H4) samples were obtained.

2.3. Sample characterization

The powder X-ray diffraction (XRD) patterns of the samples were obtained using a DX-2700 diffractometer in the scanning angle range of 5–80°. DSC curves of the samples were measured by DSC131 thermal analyzer (Setaram, California, France). The samples were tested from 50 to 500 °C with heating rates of 5, 10, 15, and 20 °C·min^{-1} under high-purity nitrogen. Use Netzsch STA449F3 (TG) to detect the samples at a heating rate of 10°C min^{-1} in a temperature range of 40–500°C and under an argon flow of 80 ml min^{-1}. At the same time, a quadrupole mass spectrum (QMS) was recorded on the Netzsch QMS403C device.

2.4. Theoretical analysis

Draft

© The Author(s) or their Institution(s)

When describing the reaction kinetics problem (1),[31,32]

$$A'^{(s)} \rightarrow B'^{(s)} + C'(g) \qquad (1)$$

two commonly forms of equations are used, differential (2) and integral (3) form

$$\frac{d\alpha}{dt} = kf(\alpha) \qquad (2)$$

$$G(\alpha) = kt \qquad (3)$$

In the formula, t is the time, α is the reaction fraction of substance A at t. For the DSC curve, α value is equal to H_t/H_0, H_t is the reaction heat of the substance at t, which is equivalent to the part of the area under the DSC curve, and H_0 is the total exothermic heat of the substance reaction, which is equivalent to the total area of the DSC curve, k is the reaction rate constant, and $f(\alpha)$ and $G(\alpha)$ are the kinetic mechanism functions in the differential form and the integral form, respectively. The relationship between K and reaction temperature is expressed by the Arrhenius Equation:

$$k = Ae^{\left(-\frac{E}{RT}\right)} \qquad (4)$$

In this equation, A is the apparent exponential factor, E is the apparent activation energy, and R is the molar gas constant.

In non-isothermal conditions,

$$T = T_0 + \beta t \qquad (5)$$

T_0 is the temperature at which the DSC curve deviates from the baseline, and β is the constant heating rate, from Equation (2)-(5), the dynamic differential equation is available.[33]

$$\frac{d\alpha}{dT} = \frac{A}{\beta} f(\alpha) e^{\left(-\frac{E}{RT}\right)} \qquad (6)$$

Its integral form is:

Draft

© The Author(s) or their Institution(s)

$$G(\alpha) = \int_0^{\alpha} \frac{d\alpha}{f(\alpha)} \quad (7)$$

The kinetic analysis of solid-state reactions is challenging. In terms of kinetic parameters, including activation energy (E_a), pre-exponential factor (A) and kinetic model ($f(\alpha)$), each individual process should be determined as a whole complete kinetic description of the reaction. There are a large number of analytical methods that can be used to determine the kinetic parameters of discrete solid-state reactions[53-55]. For example, Djalal Trache et al. used four isoconversion models (Kissinger–Akahira–Sunose, Flynn–Wall–Ozawa, Trache–Abdelaziz–Siwani, and Vyazovkin) to accurately evaluate the kinetics triplets[33-35, 52, 56-57]. And many scholars use the model matching method to study energetic materials' thermal dynamic[32, 58-59]. In this paper, the model matching method is used to conduct thermal analysis on the typical ammonium perchlorate-based molecular perovskite energetic materials.

2.4.1 The Kissinger method

The Kissinger method is Equation (8) [60-61]

$$ln\left(\frac{\beta_i}{T_{pi}^2}\right) = ln\frac{A_k R}{E_k} - \frac{E_k}{R}\frac{1}{T_{pi}} \quad (8)$$

Plot $\frac{1}{T_{pi}}$ from $ln\left(\frac{\beta_i}{T_{pi}^2}\right)$ to get a straight line. Get E_k from the slope of the straight line and A_k from the intercept.

2.4.2 The Flynn-Wall-Ozawa method

The F-W-O method avoids the choice of the reaction mechanism function and directly obtains the activation energy, which is a prominent advantage of the F-W-O method. The integral form of F-W-O method is represented by Equation (9) [62].

$$lg\beta = \lg\left(\frac{AE}{RG(\alpha)}\right) - 2.315 - 0.4567\frac{E}{RT_p} \quad (9)$$

Since each of the peak top temperatures T_{pi} of different β_i is approximately equal to each α, *lgβ-1/T* can be used to determine the *E* value.

2.4.3 The Šatava-Šesták method

The Šatava-Šesták method is suitable for the study of non-isothermal solid-phase thermal decomposition kinetics. Because the derivation is rigorous and the judgment is well-founded, the

© The Author(s) or their Institution(s)

results obtained by this method are generally more reasonable. The Šatava-Šesták method is represented by Equation (10)[63].

$$lgG(\alpha) = \lg\left(\frac{A_s E_s}{R\beta}\right) - 2.315 - 0.4567\frac{E_s}{RT_p} \quad (10)$$

The $G(\alpha)$ in formula (10) is taken from the integral form of 30 given in the literature[64]. For fixed β_i, $\lg\left(\frac{A_s E_s}{R\beta}\right)$ is a constant, so $lgG(\alpha)$-$1/T$ can be used to determine each *Es* value and *As* value. The judgment conditions are $0<Es<400$ kJ·mol^{-1}, $|(Eo-Es/Eo)|\leq 0.1$, and $|(\frac{lgAs - lgA_k}{lgA_k})|\leq 0.2$.

2.4.4. Thermodynamic analysis

Putting the heating rate data into Equation (11) and (12)[59, 65], the thermal decomposition extrapolation starting temperature T_{e0}, peak top temperature T_{P0}, thermal ignition temperature T_{eb}, and heat explosion temperature T_{pb} can be obtained.

$$T_{e0\ or\ p0} = T_{ei\ or\ pi} + b\beta_i + c\beta_i^2 + d\beta_i^3 \quad (11)$$

$$T_{eb\ or\ pb} = \frac{E - \sqrt{E^2 - 4ERT_{e0\ or\ p0}}}{2R} \quad (12)$$

And then put the obtained Es, as into Equation (13), (14), and (15) to get enthalpy (ΔH), entropy (ΔS) and Gibbs free energy (ΔG)[59].

$$Ae^{\left(\frac{-E}{RT}\right)} = \upsilon e^{\left(\frac{-\Delta G}{RT}\right)} = \frac{k_B T}{h} e^{\left(\frac{-\Delta G}{RT}\right)} \quad (13)$$

$$\Delta G = \Delta H - T\Delta S \quad (14)$$

$$\Delta H = E - RT \quad (15)$$

In the formula, T is the experimental temperature(K), R is the molar gas constant (8.314 J mol^{-1} K^{-1}), h is the Planck constant (6.625×10^{-34}J s), k_B is the Boltzmanm constant, (1.3807×10^{-23}J K^{-1}) and υ is the Einstein vibration frequency.

3.Result and Discussion

The powder XRD patterns of the AP-based molecular perovskite energetic material samples are shown in Fig. 1, which are highly consistent with the simulated powder XRD pattern (CCDC: 1528108, 1956805, 1956806, 1956807). The crystal structures of samples were also shown as insert images.

Draft

© The Author(s) or their Institution(s)

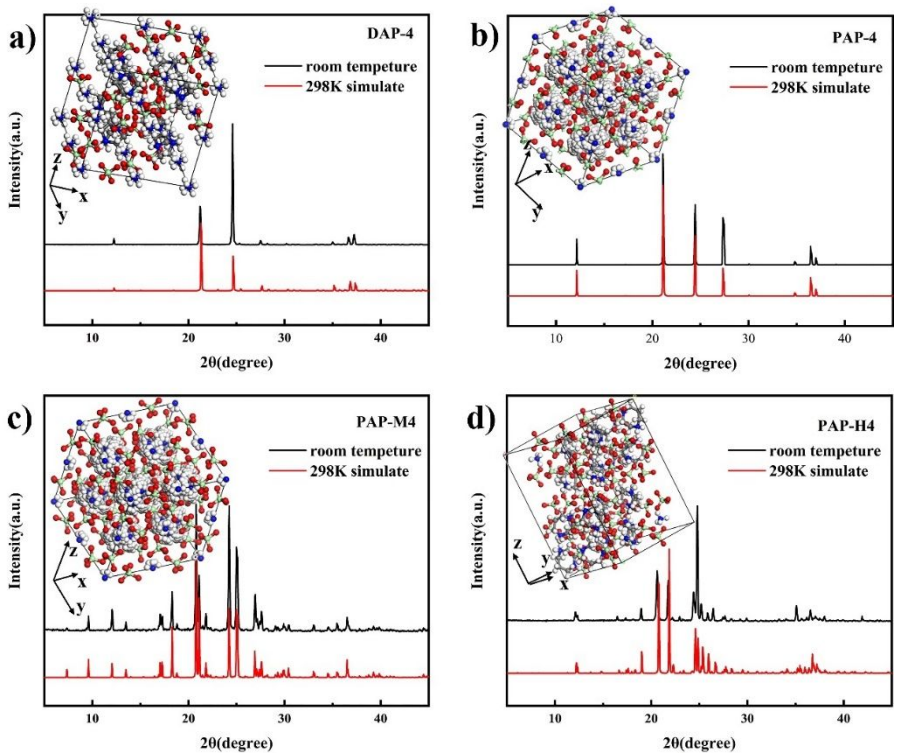

Fig. 1. P-XRD patterns of AP-based molecular perovskite energetic materials.

3.1 Thermal Decomposition of AP-based molecular perovskite energetic materials

The DSC curve at different heating rates and TG curve at 10k min^{-1} of AP-based molecular perovskite energetic materials are shown in Fig. 2 and Fig. 3. From the DSC curve, we can see that each perovskite molecule has two peaks. And the first peak corresponding to the TG curve has no significant mass loss, which revealed that phase transition process appeared. For the second peak, the TG curve has a significant mass loss, indicating that a thermal decomposition reaction has occurred. Table 1 lists the experimental data of thermal analysis at this stage by DSC curves. It is obviously found that AP-based molecular perovskite energetic materials have good thermal stability.

3.2 Non-isothermal kinetics of AP-based molecular perovskite energetic materials

In Fig. 2, as the heating rate increases, the thermal decomposition curve shifts to higher temperatures. The thermal decomposition kinetics of AP-based molecular perovskite energetic materials were analyzed by Kissinger method and Ozawa method. The E_k and lgA_k of DAP-4 calculated by Kissinger method are 205.4 kJ mol^{-1} and 15.7 min^{-1}, respectively. The Kissinger method can roughly estimate the activation energy

© The Author(s) or their Institution(s)

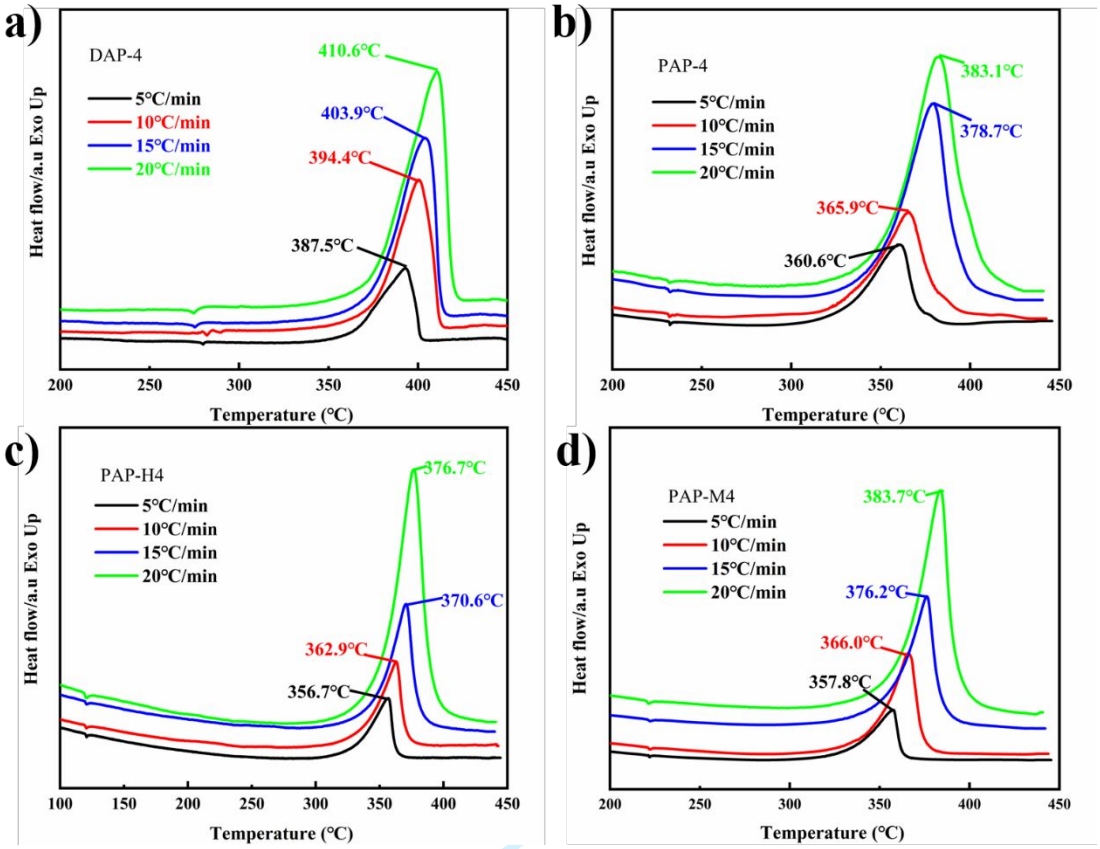

Fig. 2. DSC curves of (a) DAP-4, (b) PAP-4, (c)PAP-H4, and (d) PAP-M4 at different heating rates.

of thermal decomposition with the peak value of the non-isothermal curve. And the activation energy of DAP-4 calculated by the FWO method is 206 kJ·mol^{-1}. Therefore, the results are found to be credible. Table 2 shows the calculation results obtained by DAP-4 and the other three ap-based analysis methods. The activation energy of PAP-H4 is the highest at 218.2 kJ·mol^{-1}, while the activation energy of PAP-M4 and PAP-4 are lower at 170.1 and 181.7 kJ·mol^{-1}, respectively.

In order to obtain the most probable mechanism function $G(\alpha)$ from the non-isothermal DSC curves, the Šatava-Šesták method of strict derivation and it was well found that judgment is used. Since the reaction process α (Supporting information Table S1-S4) is easily affected by the noise of the baseline and the instrument, the α fluctuates greatly between 0-0.1 and 0.9-1. The judgment condition $|(Eo\text{-}Es/Eo)|\leq 0.1$ is changed to $|(Eo\text{-}Es/Eo)|\leq 0.15$, and add the conditions that the linear correlation coefficient of the calculation result is greater than 0.99 and the standard deviation is

© The Author(s) or their Institution(s)

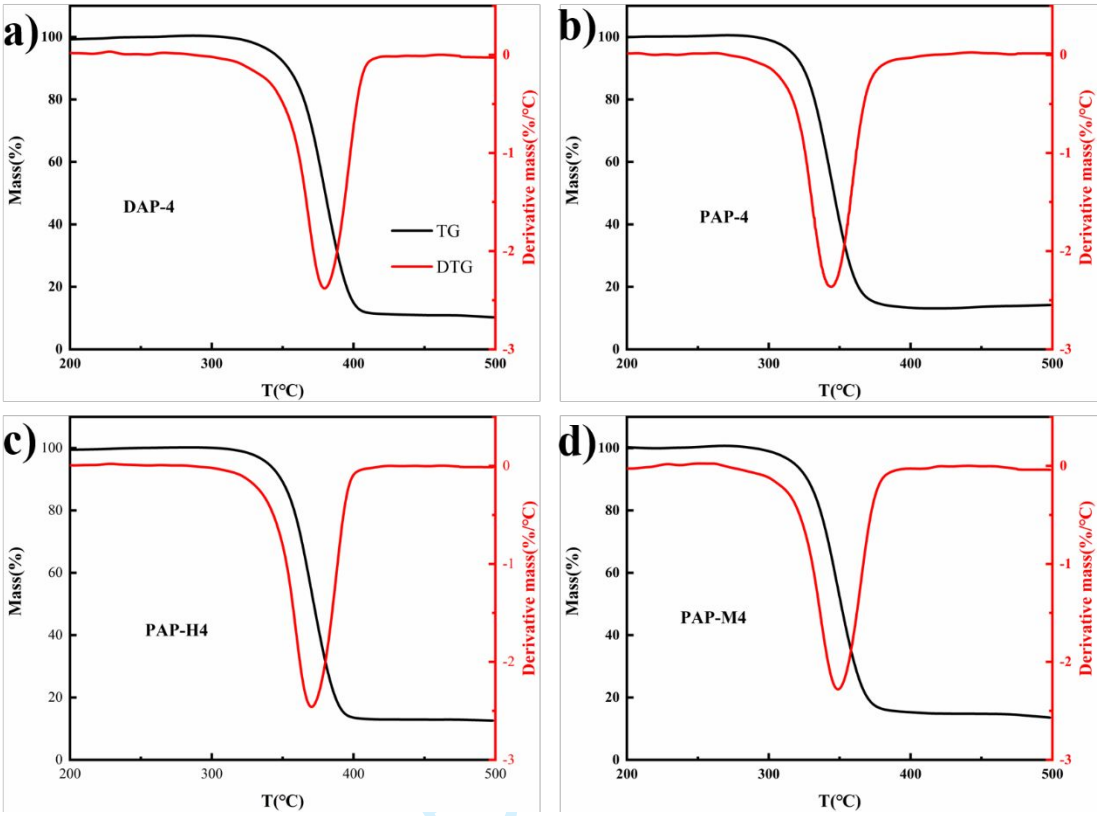

Fig. 3. TG and DTG curves for the thermal decomposition of AP-based molecular perovskite energetic materials at 10k·min^{-1}.

less than 0.03. If $G(\alpha)$ meets the above conditions, it is inferred that $G(\alpha)$ can be regarded as the probable mechanism function of thermal decomposition.

Table 3 shows the kinetic parameters calculated by the Satava–Sestak method for the thermal decomposition of DAP-4. At that stage, by comparing the activation energy values calculated by the FWO method and the Šatava-Šesták method, and the pre-exponential factors calculated by the Kissinger method and the Šatava-Šesták method, the most likely Mechanism Function is to determine Mechanism Function[10, 28, 47]. But after calculating the correlation coefficient and the residual variance value, it is found that only Mechanism Function 10, as shown in Table 3, meets the above conditions. Therefore, we can conclude that the reaction mechanism of DAP-4 decomposition is random nucleation and subsequent growth reactions. Its Mechanism Function is $G(\alpha) = [-ln\,(1-\alpha)]^{\frac{2}{3}}$ and $f(\alpha) = \frac{3}{2}(1-\alpha)[-ln\,(1-\alpha)]^{\frac{1}{3}}$. And the Es and As of thermal decomposition of DAP-4 are 232.9 kJ mol^{-1} and 1.0×10^{18} min^{-1}, respectively.

© The Author(s) or their Institution(s)

Table 1. Characteristic Parameters of DSC Experiments of AP-based molecular perovskite energetic materials.

sample	β (°C·min^{-1})	T_{onset} (°C)	T_{Peak} (°C)	T_{offset} (°C)	ΔHr (J·g^{-1})
DAP-4	5	361.2	387.5	395.8	3870.2
	10	369.5	394.3	405.8	4066.7
	15	377.0	403.9	412.6	3918.8
	20	379.4	410.6	418.9	3322.6
PAP-4	5	338.8	360.6	370.5	2626.8
	10	343.2	365.9	379.7	2514.9
	15	350.5	378.7	392.0	2750.0
	20	352.1	383.1	399.8	2621.5
PAP-H4	5	336.4	356.7	361.6	2621.2
	10	341.8	362.9	369.7	2735.1
	15	348.6	370.6	379.4	2750.2
	20	351.1	376.7	389.5	2865.4
PAP-M4	5	340.0	357.8	362.1	2276.9
	10	349.8	366.0	373.6	2321.2
	15	358.1	376.2	383.8	1618.0
	20	362.8	383.7	391.5	2386.0

Table 2. The activation energy of AP-based molecular perovskite energetic materials by Kissinger and FWO method.

Sample	Kissinger			FWO		
	E_k(kJ·mol^{-1})	lgA_k	R^2	Eo(kJ·mol^{-1})	lgA	R^2
DAP-4	205.4±4.8	15.7	0.9758	206±0.9	12.2	0.9782
PAP-M4	167.9±3.2	13.3	0.98	170.1±0.6	11.1	0.9823
PAP-H4	218.8±4.7	17.7	0.9781	218.2±0.8	13	0.9801
PAP-4	178.5±7.1	14.2	0.9562	181.7±1.2	11.4	0.9607

The thermal decomposition kinetic Mechanism Functions of PAP-4, PAP-M4 and PAP-H4 were deduced by the same method. The results are shown in Table **S5-S7** in

Draft

© The Author(s) or their Institution(s)

Supporting Information, it is concluded that PAP-4, PAP-H4 and DAP-4 are consistent with Mechanism Function 10, and PAP-M4 is consistent with Mechanism Function 11.

Table 3. Values of activation energy and pre-exponential factor obtained for the thermal decomposition of DAP-4 from the Šatava-Šesták method

No.	β=5 K·min^{-1}			β=10 K·min^{-1}			β=15 K·min^{-1}			β=20 K·min^{-1}		
	Es(KJ/mol)	LgAs	r	Es(KJ/mol)	LgAs	r	Es(KJ/mol)	LgAs	r	Es(KJ/mol)	LgAs	r
1	540.1	43.19	0.9908	513.1	40.37	0.9942	532.4	41.45	0.9948	538.3	41.57	0.9892
2	585.0	46.74	0.9963	555.1	43.64	0.9981	574.6	44.69	0.9985	582.6	44.95	0.9952
3	604.6	47.77	0.9980	573.7	44.57	0.9992	592.7	45.56	0.9995	602.0	45.91	0.9972
4	645.3	51.26	0.9996	612.9	47.89	0.9995	630.4	48.71	0.9999	642.5	49.27	0.9993
5	161.3	12.24	0.9996	153.2	11.41	0.9995	157.6	11.61	0.9999	160.6	11.74	0.9993
6	153.9	11.70	0.9987	146.1	10.91	0.9996	150.7	11.13	0.9998	153.2	11.23	0.9980
7	500.2	38.79	0.9862	476.1	36.26	0.9910	494.3	37.27	0.9914	499.2	37.34	0.9842
8	463.2	35.59	0.9804	441.8	33.32	0.9867	458.8	34.27	0.9868	462.9	34.30	0.9780
9	356.5	28.50	0.9975	339.6	26.73	0.9947	346.2	26.93	0.9964	354.9	27.40	0.9979
10	237.7	18.74	0.9975	226.4	17.57	0.9947	230.8	17.69	0.9964	236.6	18.00	0.9979
11	178.3	13.89	0.9975	169.8	13.02	0.9947	173.1	13.11	0.9964	177.4	13.34	0.9979
12	118.8	9.10	0.9975	113.2	8.52	0.9947	115.4	8.58	0.9964	118.3	8.73	0.9979
13	1426.1	117.36	0.9975	1358.5	110.22	0.9947	1384.7	111.02	0.9964	1419.5	112.92	0.9979
14	89.1	6.74	0.9975	84.9	6.31	0.9947	86.5	6.36	0.9964	88.7	6.46	0.9979
15	713.1	58.02	0.9975	679.3	54.46	0.9947	692.4	54.86	0.9964	709.7	55.80	0.9979
16	1069.6	87.67	0.9975	1018.9	82.32	0.9947	1038.6	82.91	0.9964	1064.6	84.34	0.9979
17	307.8	24.05	0.9987	292.2	22.44	0.9996	301.4	22.91	0.9998	306.5	23.11	0.9980
18	181.7	14.11	0.9376	174.8	13.35	0.9502	182.1	13.77	0.9510	182.6	13.68	0.9340
19	217.0	16.93	0.9652	207.3	15.91	0.9735	216.0	16.41	0.9745	217.1	16.35	0.9622
20	156.5	12.09	0.9116	151.4	11.51	0.9277	157.6	11.86	0.9282	157.8	11.77	0.9079
21	322.7	25.15	0.9996	306.5	23.47	0.9995	315.2	23.87	0.9999	321.2	24.15	0.9993
22	330.6	25.70	0.9997	314.2	23.99	0.9990	322.5	24.36	0.9995	329.1	24.67	0.9995
23	270.0	21.15	0.9908	256.5	19.75	0.9942	266.2	20.28	0.9948	269.2	20.34	0.9892
24	405.0	32.14	0.9908	384.8	30.04	0.9942	399.3	30.84	0.9948	403.8	30.93	0.9892
25	135.0	10.28	0.9908	128.3	9.59	0.9942	133.1	9.85	0.9948	134.6	9.87	0.9892
26	90.0	6.73	0.9908	85.5	6.28	0.9942	88.7	6.44	0.9948	89.7	6.46	0.9892
27	67.5	4.99	0.9908	64.1	4.66	0.9942	66.6	4.78	0.9948	67.3	4.79	0.9892
28	220.0	17.88	0.7686	218.2	17.52	0.7233	200.4	15.84	0.7639	218.8	17.18	0.7751
29	490.1	39.88	0.9561	474.8	38.11	0.9339	466.6	36.95	0.9560	487.9	38.37	0.9596
30	110.0	8.69	0.7389	109.1	8.51	0.7233	100.2	7.69	0.7639	109.4	8.34	0.7751

It can be seen that the decomposition of AP-based molecular perovskite energetic materials belongs to random nucleation and growth following model, and the mechanism function of PAP-M4 belongs to $G(\alpha) = [-ln(1-\alpha)]^{\frac{1}{2}}$ and $f(\alpha) = 2(1-\alpha)[-ln(1-\alpha)]^{\frac{1}{2}}$. Therefore, the activation energy and pre-exponential factor of PAP-4 are 171.3 kJ·mol^{-1} and 4.05×10^{13} min^{-1}, respectively. The *Es* and *As* of PAP-H4 are 205.0 kJ·mol^{-1} and 4.08×10^{16} min^{-1}, respectively. The activation energy and pre-exponential factor of PAP-M4 are 179.1 kJ·mol^{-1} and 2.08×10^{14} min^{-1}, respectively.

Draft

© The Author(s) or their Institution(s)

According to the mechanism of thermal decomposition, we also use coupled thermal analysis technology TG-QMS to analyze the entire decomposition process. TG-QMS proved to be an effective method to study the mechanism of thermal decomposition, it can better understand thermal degradation and reaction mechanisms by measuring the gas evolution curve of the decomposition products[38]. As shown in the Fig. 4, it can see the formation of H_2O, NO_2, CO_2 in the decomposition reaction. Therefore, it can be inferred that when AP-based molecular perovskite energetic materials receive external heating, the protons in A-sites (H_2dabco^{2+}, H_2pz^{2+}, H_2mpz^{2+}, and H_2hpz^{2+}) are activated, but the anion skeletons are maintained by the Coulomb forces. When the temperature reaches a certain temperature, the external energy is greater than the Coulomb force between $ClO_4^-$and NH_4^+, the anion skeleton will be destroyed, and the activated protons and ClO_4^- form a large amount of $HClO_4$. At the same time, $HClO_4$ is promoted by the electron flow at the A-sites and the lower activation energy of the substance itself to promote reductive decomposition, the generated superoxide radical $\cdot O_2^-$ reacts with the organic fuel at the A-sites to generate H_2O, NO_2, CO_2, etc. Because of the unique molecular perovskite structure that combines the oxidizer and the fuel, so that AP-based molecular perovskite energetic materials obtain a greater exothermic energy.

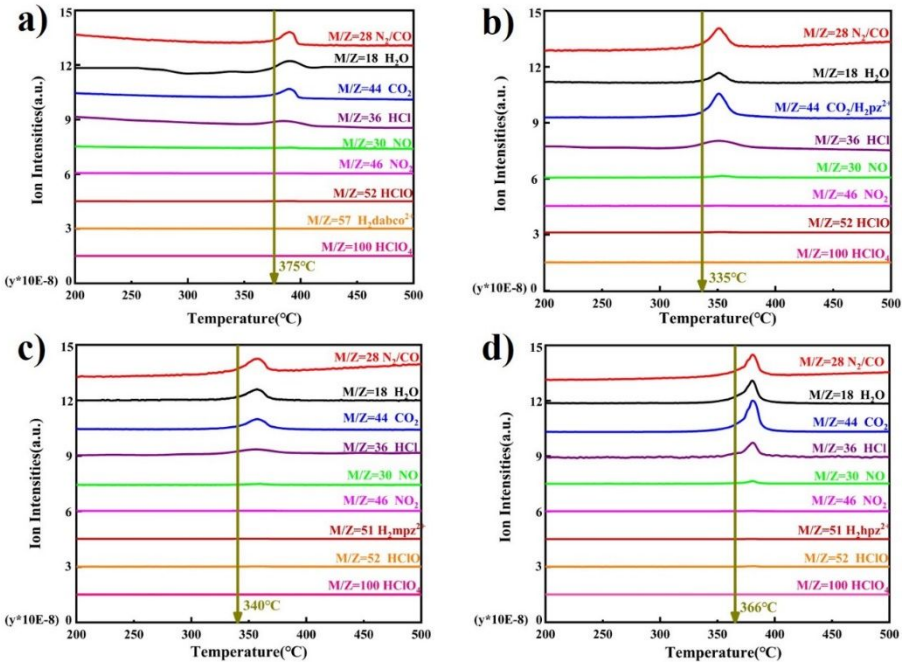

© The Author(s) or their Institution(s)

Fig. 4. the mass spectra for AP-based molecular perovskite energetic materials: (a)DAP-4, (b) PAP-4, (c) PAP-M4, (d) PAP-H4 at a heating rate of 10 °C·min^{-1}.

3.3 Thermodynamic parameters

Putting the heating rate data (Table 1) into equation (11) and (12), the thermal decomposition extrapolation starting temperature T_{e0}, peak top temperature T_{P0}, thermal ignition temperature T_{eb}, and heat explosion temperature T_{pb} of AP-based molecular perovskite energetic materials can be obtained. And then put the obtained *Es, As,* T_{p0} into equation (13)-(15) to get enthalpy (ΔH), entropy (ΔS) and Gibbs free energy (ΔG) of AP-based molecular perovskite energetic materials, the results are listed in Table 4. It is concluded from Table 4 that the T_{e0}, T_{P0}, T_{eb}, and T_{pb} of AP-based molecular perovskite energetic materials are relatively high (300 °C-405 °C), and the values enthalpy (ΔH), entropy (ΔS) and Gibbs free energy (ΔG) of AP-based molecular perovskite energetic materials are all greater than 0, indicating that they are generally thermodynamically stable.

Table 4. Thermodynamic parameters of AP-based molecular perovskite energetic materials

sample	T_{e0}(°C)	T_{eb}(°C)	T_{P0}(°C)	T_{pb}(°C)	$\triangle S$ J(mol·k)$^{-1}$	$\triangle H$ (kJ·mol^{-1})	$\triangle G$ (kJ·mol^{-1})
DAP-4	356.4	371.2	388.6	405.0	84.54	227.40	171.45
PAP-4	345.9	365.7	378.6	400.6	14.03	165.88	156.74
PAP-H4	338.1	354.1	355.1	371.9	58.56	199.78	162.99
PAP-M4	330.8	348.8	356.1	376.9	8.86	162.8	157.25

3.4 Thermal safety prediction

The maximum reaction rate arrival time of the runaway reaction (TM_{Rad}) is usually used to determine the thermal safety of the material during storage or transportation[47]. In this thermal analysis test, the sample preparation method of the DSC131 EVO differential scanning calorimeter is the crucible compression sample preparation. There is only energy exchange with the outside world, no material exchange, which is approximately equivalent to a closed environment. Through Equations (16)-(18) reaction heat (ΔH_r), heat capacity (c_p) and reaction rate (α), TMR_{ad} of AP-based molecular perovskite energetic materials can be obtained[47].

© The Author(s) or their Institution(s)

$$\alpha = \frac{H_t}{H_0} \tag{16}$$

$$\Delta T_{ad} = \frac{\Delta H_r}{c_p} \tag{17}$$

$$\frac{dT}{dt} = \frac{1}{\varphi}\Delta T_{ad}\frac{d\alpha}{dt} \tag{18}$$

The thermal analysis software AKTS derives the relationship between the initial temperature of DAP-4 and the corresponding adiabatic induction time as shown in Fig. 5a. The specific heat capacity c_p used for calculation is 1.226 $J^{-1}\cdot g^{-1}\cdot k^{-1}$. As shown in Figure 5a, the values of T_{D2}, T_{D4}, T_{D8} and T_{D24} of DAP-4 are 275.7, 267.2, 259 and 246.6°C, respectively. Generally, T_{D24} is used as a reference for operating temperature, the T_{D24} of PAP-4, PAP-M4 and PAP-H4 are 201.2, 194.5 and 217.5°C, respectively. It can be seen that under adiabatic conditions, T_{D24} is much lower than the thermal decomposition temperature obtained in DSC. The T_{D24} of the current excellent energetic material TKX-50 is 168°C[47], which shows that the thermal safety of AP-based molecular perovskite energetic materials is better.

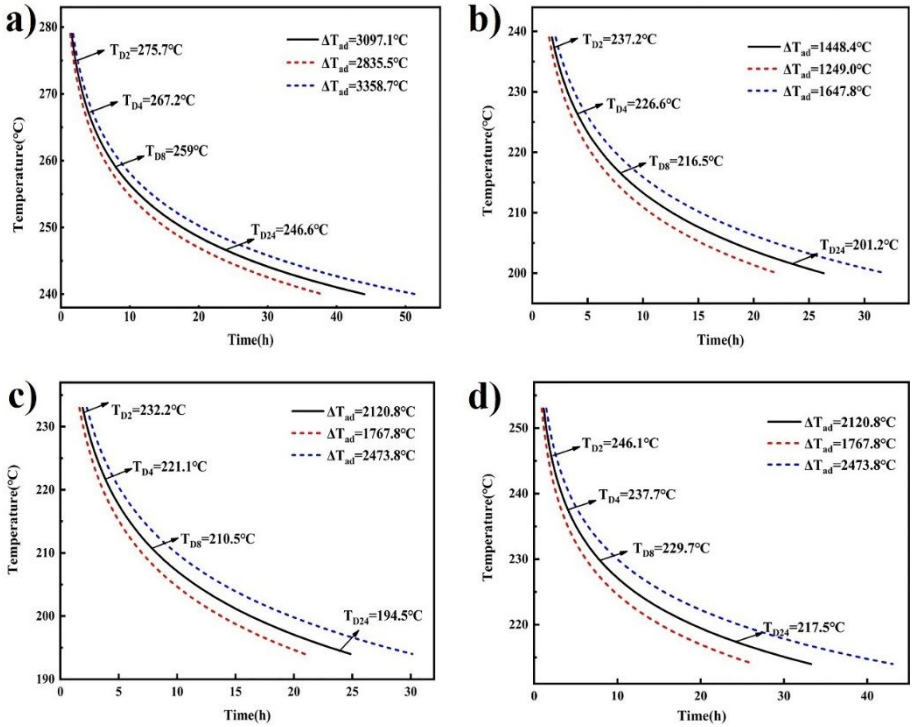

Fig. 5. The curves of critical onset temperature versus adiabatic induction time TMR_{ad} of (a) DAP-4, (b) PAP-4, (c) PAP-M4, and (d) PAP-H4.

4. Conclusion

© The Author(s) or their Institution(s)

In summary, the thermal kinetics, thermodynamics, and decomposition mechanism of four typical AP-based molecular perovskite energetic materials, DAP-4, PAP-4, PAP-M4, and PAP-H4, were studied, and their thermal safety performance was estimated. The decomposition temperatures were measured by DSC, and the activation energy, the thermal decomposition extrapolation temperature, the thermal ignition temperature and the thermal explosion temperature of the four substances were calculated. The calculation shows that the thermal stabilities of AP-based molecular perovskite energetic materials are very excellent, indicating that they have a very high application prospect. And the dynamic mechanism of AP-based molecular perovskite energetic materials was analyzed. They all follow the random nucleation and growth model. The Mechanism Functions of DAP-4, PAP-4, and PAP-H4 are $G(\alpha) = [-ln(1-\alpha)]^{\frac{2}{3}}$ and $f(\alpha) = \frac{3}{2}(1-\alpha)[-ln(1-\alpha)]^{\frac{1}{3}}$. The Mechanism Function of PAP-M4 belongs to $G(\alpha) = [-ln(1-\alpha)]^{\frac{1}{2}}$ and $f(\alpha) = 2(1-\alpha)[-ln(1-\alpha)]^{\frac{1}{2}}$. Coupled TG-QMS was used to provide their decomposition mechanism. In addition to thermal dynamic analysis, their thermal safety performance was also evaluated. The T_{D24} of DAP-4, PAP-4, PAP-M4 and PAP-H4 are 246.6, 201.2, 194.5 and 217.5 °C, respectively. It can be found that PAP-M4 and PAP-4 have the lower T_{D24} and poor stability, while DAP-4 and PAP-H4 have higher T_{D24} and are more stable under adiabatic storage.

This work offered an important understanding of the decomposition of AP-based molecular perovskite energetic materials, and had guiding significance for its safe storage and subsequent applications.

AUTHOR INFORMATION

Corresponding Author

*** Tel: +86 0351 3920630. Fax: +86 0351 3920630. E-mail: TanYXnuc@163.com (Y. T).**

***Tel: +86 0351 3920630. Fax: +86 0351 3920630. E-mail: nash_deng@163.com (P. D).**

Notes

© The Author(s) or their Institution(s)

The authors declare no competing financial interest.

ACKNOWLEDGMENTS

We acknowledge the National Natural Science Foundation of China (No. 21975227).

Draft

© The Author(s) or their Institution(s)

Reference

1. Badgujar, D. M.; Talawar, M. B.; Asthana, S. N.; Mahulikar, P. P., Advances in science and technology of modern energetic materials: An overview. *J Hazard Mater* **2008,** *151* (2-3), 289-305. https://doi.org/10.1016/j.jhazmat.2007.10.039

2. S. Manzoor, Q. T., X. Yin, J. Zhang, Nitro-tetrazole based high performing explosives: recent overview of synthesis and energetic properties. *Def Technol* **2021**. https://doi.org/ 10.1016/j.dt.2021.02.002

3. S. Loebbecke, M. B., A. Pfeil, A. Krause In *Thermal behavior and stability of HNIW(CL20)*, Int Annu Conf ICT, 1998; pp 1-15.

4. Ordzhonikidze, O.; Pivkina, A.; Frolov, Y.; Muravyev, N.; Monogarov, K., Comparative study of HMX and CL-20. *J Therm Anal Calorim* **2011,** *105* (2), 529-534. https://doi.org/10.1007/s10973-011-1562-1

5. Yu, L.; Jiang, X. B.; Guo, X. Y.; Ren, H.; Jiao, Q. J., Effects of binders and graphite on the sensitivity of epsilon-HNIW. *J Therm Anal Calorim* **2013,** *112* (3), 1343-1349. https://doi.org/10.1007/s10973-012-2679-6

6. Boddu, V. M.; Viswanath, D. S.; Ghosh, T. K.; Damavarapu, R., 2,4,6-Triamino-1,3,5-trinitrobenzene (TATB) and TATB-based formulations-A review. *J Hazard Mater* **2010,** *181* (1-3), 1-8. https://doi.org/10.1016/j.jhazmat.2010.04.120

7. Qu, Y. Y.; Babailov, S. P., Azo-linked high-nitrogen energetic materials. *J Mater Chem A* **2018,** *6* (5), 1915-1940. https://doi.org/10.1039/C7TA09593G

8. Chen, S. L.; Yang, Z. R.; Wang, B. J.; Shang, Y.; Sun, L. Y.; He, C. T.; Zhou, H. L.; Zhang, W. X.; Chen, X. M., Molecular perovskite high-energetic materials. *Sci China Mater* **2018,** *61* (8), 1123-1128. https://doi.org/10.1007/s40843-017-9219-9

9. Chen, S. L.; Shang, Y.; He, C. T.; Sun, L. Y.; Ye, Z. M.; Zhang, W. X.; Chen, X. M., Optimizing the oxygen balance by changing the A-site cations in molecular perovskite high-energetic materials. *Crystengcomm* **2018,** *20* (46), 7458-7463. https://doi.org/10.1039/C8CE01350K

10. Shang, Y.; Yu, Z. H.; Huang, R. K.; Chen, S. L.; Liu, D. X.; Chen, X. X.; Zhang, W. X.; Chen, X. M., Metal-Free Hexagonal Perovskite High-Energetic Materials with $NH_3OH^+/NH_2NH_3^+$ as B-Site Cations. *Engineering-Prc* **2020,** *6* (9), 1013-1018.

Draft

© The Author(s) or their Institution(s)

https://doi.org/10.1016/j.eng.2020.05.018

11. Jia, Q.; Bai, X. Y.; Zhu, S. Y.; Cao, X.; Deng, P.; Hu, L. S., Fabrication and characterization of Nano (H_2dabco)[$K(ClO_4)_3$] molecular Perovskite by ball milling. *J Energ Mater* **2020,** *38* (4), 377-385. https://doi.org/10.1080/07370652.2019.1698675

12. Jia, Q.; Deng, P.; Li, X. X.; Hu, L. S.; Cao, X., Insight into the thermal decomposition properties of potassium perchlorate ($KClO_4$)-based molecular perovskite. *Vacuum* **2020,** *175*. https://doi.org/10.1016/j.vacuum.2020.109257

13. Shang, Y.; Huang, R. K.; Chen, S. L.; He, C. T.; Yu, Z. H.; Ye, Z. M.; Zhang, W. X.; Chen, X. M., Metal-Free Molecular Perovskite High-Energetic Materials. *Cryst Growth Des* **2020,** *20* (3), 1891-1897. https://doi.org/10.1016/j.eng.2020.05.018

14. W. Zhang, S. C., Y. Shang, et al., Molecular perovskites as a new platform for designing advanced multi-component energetic crystals. *Energetic Materials Frontiers* **2020,** *1*, 123-135. https://doi.org/10.1016/j.enmf.2020.12.003

15. Deng, P.; Jiao, Q. J.; Ren, H., Synthesis of nitrogen-doped porous hollow carbon nanospheres with a high nitrogen content: A sustainable synthetic strategy using energetic precursors. *Sci Total Environ* **2020,** *714*. https://doi.org/10.1016/j.scitotenv.2020.136725

16. Deng, P.; Ren, H.; Jiao, Q., Enhanced the combustion performances of ammonium perchlorate-based energetic molecular perovskite using functionalized graphene. *Vacuum* **2019,** *169*. https://doi.org/10.1016/j.vacuum.2019.108882

17. Deng, P.; Wang, H.; Yang, X.; Ren, H.; Jiao, Q., Thermal decomposition and combustion performance of high-energy ammonium perchlorate-based molecular perovskite. *Journal of Alloys & Compounds* **2020**, 154257. https://doi.org/10.1016/j.jallcom.2020.154257

18. Zhou, J.; Ding, L.; Zhao, F.; Wang, B.; Zhang, J., Thermal studies of novel molecular perovskite energetic material ($C_6H_{14}N_2$) $NH_4(ClO_4)_3$). *Chinese Chemical Letters* **2020,** *31* (2), 554-558. https://doi.org/10.1016/j.cclet.2019.05.008

19. Ravindran, T. R.; Rajan, R.; Venkatesan, V., Review of Phase Transformations in Energetic Materials as a Function of Pressure and Temperature. *J Phys Chem C* **2019,** *123* (48), 29067-29085. https://doi.org/10.1021/acs.jpcc.9b04885

Draft

© The Author(s) or their Institution(s)

20. Han, K. H.; Zhang, X. M.; Deng, P.; Jiao, Q. J.; Chu, E. Y., Study of the thermal catalysis decomposition of ammonium perchlorate-based molecular perovskite with titanium carbide MXene. *Vacuum* **2020,** *180*. https://doi.org/10.1016/j.vacuum.2020.109572

21. Liu, Y.; Hu, L. S.; Gong, S. D.; Guang, C. Y.; Li, L. Q.; Hu, S. Q.; Deng, P., Study of Ammonium Perchlorate-based Molecular Perovskite $(H_2dabco)[NH_4(ClO_4)_3]$/Graphene Energetic Composite with Insensitive Performance. *Cent Eur J Energ Mat* **2020,** *17* (3), 451-469. https://doi.org/10.22211/cejem/127934

22. Deng, P.; Jiao, Q. J.; Ren, H., Laminated ammonium perchlorate-based composite prepared by ice-template freezing-induced assembly. *J Mater Sci* **2021,** *56* (3), 2077-2087. https://doi.org/10.1007/s10853-020-05174-5

23. Fang, H.; Guo, X. Y.; Shi, L. P.; Han, K. H.; Nie, J. X.; Wang, S. J.; Wu, C. C.; Deng, P., The effects of TiH2 on the thermal decomposition performances of ammonium perchlorate-based molecular perovskite (DAP-4). *J Energ Mater* **2021**. https://doi.org/10.1080/07370652.2021.1916128

24. Fang, H.; Guo, X. Y.; Wang, W.; Nie, J. X.; Han, K. H.; Wu, C. C.; Wang, S. J.; Wang, D.; Deng, P., The thermal catalytic effects of CoFe-Layered double hydroxide derivative on the molecular perovskite energetic material (DAP-4). *Vacuum* **2021,** *193*. https://doi.org/10.1016/j.vacuum.2021.110503

25. Zhu, S. D.; Cao, X.; Cao, X. Q.; Feng, Y. Q.; Lin, X. B.; Han, K. H.; Li, X. X.; Deng, P., Metal-doped (Fe, Nd, Ce, Zr, U) graphitic carbon nitride catalysts enhance thermal decomposition of ammonium perchlorate-based molecular perovskite. *Mater Design* **2021,** *199*. https://doi.org/10.1016/j.matdes.2020.109426

26. Deng, P.; Ren, H.; Jiao, Q. J., Enhanced thermal decomposition performance of sodium perchlorate by molecular assembly strategy. *Ionics* **2020,** *26* (2), 1039-1044. https://doi.org/10.1007/s11581-019-03301-0

27. A. Sikder, N. S., review of advanced high performance, insensitive and thermally stable energetic materials emerging for military and space applications. *J Hazard Mater* **2004,** *112*, 1-15. https://doi.org/10.1016/j.jhazmat.2004.04.003

28. Cheng, T. Z., Review of novel energetic polymers and binders - high energy

Draft

© The Author(s) or their Institution(s)

propellant ingredients for the new space race. *Des Monomers Polym* **2019,** *22* (1), 54-65. https://doi.org/10.1080/15685551.2019.1575652

29. Liu, G. R.; Xiong, Y.; Gou, R. J.; Zhang, C. Y., Difference in the Thermal Stability of Polymorphic Organic Crystals: A Comparative Study of the Early Events of the Thermal Decay of 2,4,6,8,10,12-Hexanitro-2,4,6,8,10,12-hexaazaisowurtzitane (CL-20) Polymorphs under the Volume Constraint Condition. *J Phys Chem C* **2019,** *123* (27), 16565-16576. https://doi.org/10.1021/acs.jpcc.9b04126

30. Ye, C. C.; An, Q.; Cheng, T.; Zybin, S.; Naserifar, S.; Ju, X. H.; Goddard, W. A., Reaction mechanism from quantum molecular dynamics for the initial thermal decomposition of 2,4,6-triamino-1,3,5-triazine-1,3,5-trioxide (MTO) and 2,4,6-trinitro-1,3,5-triazine-1,3,5-trioxide (MTO3N), promising green energetic materials. *J Mater Chem A* **2015,** *3* (22), 12044-12050. https://doi.org/10.1039/c5ta02486b

31. Yan, Q. L.; Zeman, S.; Svoboda, R.; Elbeih, A., Thermodynamic properties, decomposition kinetics and reaction models of BCHMX and its Formex bonded explosive. *Thermochim Acta* **2012,** *547*, 150-160. https://doi.org/10.1016/j.tca.2012.08.018

32. Harmen, Y.; Chhiti, Y.; Alaoui, F. E. M.; Bentiss, F.; El Khouakhi, M.; Jama, C.; Duquesne, S.; Bensitel, M.; Deshayes, L., Thermal and energetic behaviour of solid-solid-liquid phase change materials storage unit: Experimental and numerical comparative study of the top, bottom and horizontal configurations. *J Energy Storage* **2021,** *33*. https://doi.org/10.1016/j.est.2020.102025

33. Benhammada, A.; Trache, D., Green synthesis of CuO nanoparticles using Malva sylvestris leaf extract with different copper precursors and their effect on nitrocellulose thermal behavior. *J Therm Anal Calorim* **2021**. https://doi.org/10.1007/s10973-020-10469-5

34. Benhammada, A.; Trache, D.; Chelouche, S.; Mezroua, A., Catalytic Effect of Green CuO Nanoparticles on the Thermal Decomposition Kinetics of Ammonium Perchlorate. *Zeitschrift für anorganische und allgemeine Chemie* **2021,** *647* (4), 312-325. https://doi.org/https://doi.org/10.1002/zaac.202000295

35. Tarchoun, A. F.; Trache, D.; Klapötke, T. M.; Krumm, B.; Kofen, M., Synthesis

Draft

© The Author(s) or their Institution(s)

and characterization of new insensitive and high-energy dense cellulosic biopolymers. *Fuel* **2021,** *292*, 120347. https://doi.org/https://doi.org/10.1016/j.fuel.2021.120347

36. Foster, J. C.; Varlas, S.; Couturaud, B.; Coe, Z.; O'Rei'lly, R. K., Getting into Shape: Reflections on a New Generation of Cylindrical Nanostructures' Self-Assembly Using Polymer Building Blocks. *J Am Chem Soc* **2019,** *141* (7), 2742-2753. https://doi.org/10.1021/jacs.8b08648

37. Wang, F. P.; Chen, L.; Geng, D. S.; Lu, J. Y.; Wu, J. Y., Chemical reactions of a CL-20 crystal under heat and shock determined by ReaxFF reactive molecular dynamics simulations. *Phys Chem Chem Phys* **2020,** *22* (40), 23323-23332. https://doi.org/10.1039/D0CP02796K

38. T. Brill, P. G., G. Williams, Thermal decomposition of energetic materials kinetic compensation effects in HMX, RDX, and NTO. *J Phys Chem C* **1994,** *98*, 12242-12247. https://doi.org/10.1021/j100098a020

39. Zhu Shuaida, H. Z., Cao Yuqi , Xiao-xia Li, Yu-qi Feng, Xiong Cao, Peng Deng, Sandwich structure for enhancing the interface reaction of hexanitrohexaazaisowurtzitane and nanoporous carbon scaffolds film to improve the thermal decomposition performance. *Defence Technology* **2021**. https://doi.org/10.1016/j.dt.2021.08.017

40. Ye, C. C.; An, Q.; Zhang, W. Q.; Goddard, W. A., Initial Decomposition of HMX Energetic Material from Quantum Molecular Dynamics and the Molecular Structure Transition of beta-HMX to delta-HMX. *J Phys Chem C* **2019,** *123* (14), 9231-9236. https://doi.org/10.1021/acs.jpcc.9b01169

41. Deng, C.; Xue, X. G.; Chi, Y.; Li, H. Z.; Long, X. P.; Zhang, C. Y., Nature of the Enhanced Self-Heating Ability of Imperfect Energetic Crystals Relative to Perfect Ones. *J Phys Chem C* **2017,** *121* (22), 12101-12109. https://doi.org/10.1021/acs.jpcc.7b04518

42. Liu, R.; Wang, X. J.; Chen, P. W.; Kang, G.; Zhu, S. P.; Guo, Y. S., The role of tension-compression asymmetrical microcrack evolution in the ignition of polymer-bonded explosives under low-velocity impact. *J Appl Phys* **2021,** *129* (17). https://doi.org/10.1063/5.0046011

Draft

© The Author(s) or their Institution(s)

43. Liu, R.; Chen, P. W.; Zhang, X. T.; Zhu, S. P., Non-Shock Ignition Probability of Octahydro-1,3,5,7-Tetranitro-Tetrazocine-Based Polymer Bonded Explosives Based on Microcrack Stochastic Distribution. *Propell Explos Pyrot* **2020,** *45* (4), 568-580. https://doi.org/10.1002/prep.201900313

44. Bu, R. P.; Xie, W. Y.; Zhang, C. Y., Heat-Induced Polymorphic Transformation Facilitating the Low Impact-Sensitivity of 2,2-Dinitroethylene-1,1-diamine (FOX-7). *J Phys Chem C* **2019,** *123* (26), 16014-16022. https://doi.org/10.1021/acs.jpcc.9b03921

45. Xu, K. Z.; Song, J. R.; Zhao, F. Q.; Ma, H. X.; Gao, H. X.; Chang, C. R.; Ren, Y. H.; Hu, R. Z., Thermal behavior, specific heat capacity and adiabatic time-to-explosion of G(FOX-7). *J Hazard Mater* **2008,** *158* (2-3), 333-339. https://doi.org/10.1016/j.jhazmat.2008.01.077

46. Lu, Z. P.; Xue, X. G.; Meng, L. Y.; Zeng, Q.; Chi, Y.; Fan, G. J.; Li, H. Z.; Zhang, Z. M.; Nie, F. D.; Zhang, C. Y., Heat-Induced Solid-Solid Phase Transformation of TKX-50. *J Phys Chem C* **2017,** *121* (15), 8262-8271. https://doi.org/10.1021/acs.jpcc.7b00086

47. Xu, Y. B.; Tan, Y. X.; Cao, W. G.; Zhao, Y. X.; Tian, B., Thermal Decomposition Characteristics and Thermal Safety of Dihydroxylammonium 5,5 '-Bistetrazole-1,1 '-diolate Based on Microcalorimetric Experiment and Decoupling Method. *J Phys Chem C* **2020,** *124* (11), 5987-5998. https://doi.org/10.1021/acs.jpcc.0c00273

48. Cao, X.; Shang, Y. P.; Meng, K. J.; Yue, G. D.; Yang, L. Y.; Liu, Y.; Deng, P.; Hu, L. S., Fabrication of three-dimensional TKX-50 network-like nanostructures by liquid nitrogen-assisted spray freeze-drying method. *J Energ Mater* **2019,** *37* (3), 356-364. https://doi.org/10.1080/07370652.2019.1585491

49. Deng, P.; Jiao, Q. J.; Ren, H., Nano dihydroxylammonium 5,5 '-bistetrazole-1,1 '-diolate (TKX-50) sensitized by the liquid medium evaporation-induced agglomeration self-assembly. *J Energ Mater* **2020,** *38* (3), 253-260. https://doi.org/10.1080/07370652.2019.1695018

50. Yu, Q.; Liu, Y.; Sui, H. L.; Sun, J.; Li, J. S., Kinetic Analysis of Overlapping Multistep Thermal Decomposition of 2,6-Diamino-3,5-dinitropyrazine-1-oxide (LLM-105). *J Phys Chem C* **2018,** *122* (45), 25999-26006.

Draft

© The Author(s) or their Institution(s)

https://doi.org/10.1021/acs.jpcc.8b07817

51. Yu, Q.; Zhao, C. D.; Liao, L. Y.; Li, H. Z.; Sui, H. L.; Yin, Y.; Li, J. S., A mechanism for two-step thermal decomposition of 2,6-diamino-3,5-dinitropyrazine-1-oxide (LLM-105). *Phys Chem Chem Phys* **2020,** *22* (24), 13729-13736. https://doi.org/10.1039/D0CP02159H

52. Mezroua, A.; Khimeche, K.; Lefebvre, M. H.; Benziane, M.; Trache, D., The influence of porosity of ammonium perchlorate (AP) on the thermomechanical and thermal properties of the AP/polyvinylchloride (PVC) composite propellants. *J Therm Anal Calorim* **2014,** *116* (1), 279-286. https://doi.org/10.1007/s10973-013-3517-1

53. Chelouche, S.; Trache, D.; Tarchoun, A. F.; Khimeche, K., Effect of organic eutectic on nitrocellulose stability during artificial aging. *J Energ Mater* **2019,** *37* (4), 387-406. https://doi.org/10.1080/07370652.2019.1621407

54. Benhammada, A.; Trache, D.; Kesraoui, M.; Tarchoun, A. F.; Chelouche, S.; Mezroua, A., Synthesis and characterization of alpha-Fe2O3 nanoparticles from different precursors and their catalytic effect on the thermal decomposition of nitrocellulose. *Thermochim Acta* **2020,** *686*. https://doi.org/10.1016/j.tca.2020.178570

55. Hanafi, S.; Trache, D.; He, W.; Xie, W. X.; Mezroua, A.; Yan, Q. L., Thermostable Energetic Coordination Polymers Based on Functionalized GO and Their Catalytic Effects on the Decomposition of AP and RDX. *J Phys Chem C* **2020,** *124* (9), 5182-5195. https://doi.org/10.1021/acs.jpcc.9b11070

56. Trache, D.; Abdelaziz, A.; Siouani, B., A simple and linear isoconversional method to determine the pre-exponential factors and the mathematical reaction mechanism functions. *J Therm Anal Calorim* **2017,** *128* (1), 335-348. https://doi.org/10.1007/s10973-016-5962-0

57. Chelouche, S.; Trache, D.; Tarchoun, A. F.; Abdelaziz, A.; Khimeche, K.; Mezroua, A., Organic eutectic mixture as efficient stabilizer for nitrocellulose: Kinetic modeling and stability assessment. *Thermochim Acta* **2019,** *673*, 78-91. https://doi.org/10.1016/j.tca.2019.01.015

58. Yi, J. H.; Zhao, F. Q.; Xu, S. Y.; Zhang, L. Y.; Gao, H. X.; Hu, R. Z., Effects of pressure and TEGDN content on decomposition reaction mechanism and kinetics of

Draft

© The Author(s) or their Institution(s)

DB gun propellant containing the mixed ester of TEGDN and NG. *J Hazard Mater* **2009,** *165* (1-3), 853-859. https://doi.org/10.1016/j.jhazmat.2008.10.107

59. Ma, H. X.; Yan, B.; Li, Z. N.; Guan, Y. L.; Song, J. R.; Xu, K. Z.; Hu, R. Z., Preparation, non-isothermal decomposition kinetics, heat capacity and adiabatic time-to-explosion of NTO center dot DNAZ. *J Hazard Mater* **2009,** *169* (1-3), 1068-1073. https://doi.org/10.1016/j.jhazmat.2009.04.057

60. Kissinger, H., Variation of Peak Temperature with Heating Rate in Differential Thermal Analysis. *J Res Natl Bur Stand* **1956,** *57*, 217–221. https://doi.org/10.6028/jres.057.026

61. Kissinger, H., Reaction kinetic in differential thermal analysis. *Anal Chem* **1957,** *29*, 1702-1706. https://doi.org/10.1021/ac60131a045

62. Ozawa, T., A new method of analyzing thermogravimetric data. *Bull Chem soc jpn* **1965,** *38*, 1881–1886. https://doi.org/10.1246/bcsj.38.1881

63. Šesták, F. Š. J., Computer calculation of the mechanism and associated kinetic data using a non-isothermal integral method. *J Therm Anal Calorim* **1975,** *8*, 477–489. https://doi.org/10.1007/BF01910127

64. R. Hu, Q. S., *Thermal Dynamics*. 2008; Vol. 4.

65. R. Hu, Z. Y., Y. Liang, The determination of the most probable mechanism function and three kinetic parameters of exothermic decomposition reaction of energetic materials by a. *Thermochim Acta* **1988,** *123*, 135–151. https://doi.org/10.1016/0040-6031(88)80017-0

Draft

© The Author(s) or their Institution(s)